Available online at www.sciencedirect.com
SCIENCE DIRECT®

Journal of Nuclear Materials 326 (2004) 144–155

journal of nuclear materials

www.elsevier.com/locate/jnucmat

Identification of the mechanism limiting the alteration of clad spent fuel segments in aerated carbonated groundwater

C. Jégou *, S. Peuget, V. Broudic, D. Roudil, X. Deschanels, J.M. Bart

Commissariat à l' Énergie Atomique (CEA), Rhône Valley Research Center, DIEC/SESC/LMPA, BP 17171, 30207 Bagnols-sur-Cèze cedex, France

Received 13 May 2003; accepted 6 January 2004

Abstract

Leaching experiments were performed with five spent fuel samples (20 mm segments of clad fuel rods) from French power reactors (four UO_2 fuel samples with burnup ratings of 22, 37, 47 and 60 $\mathrm{GW\,d\,t_{HM}^{-1}}$ and a MOX fuel sample irradiated to 47 $\mathrm{GW\,d\,t_{HM}^{-1}}$) to determine the release kinetics of the matrix containing most of the radionuclides. The experiments were carried out with carbonated groundwater on previously leached sections of clad fuel rods in static mode, in an aerated medium at room temperature (25 °C) in a hot cell. Until 313 days of leaching and below uranium saturation, the Sr/U congruence ratios for all the UO_2 fuel samples ranged from 1 to 2; allowing for the experimental uncertainty, strontium can thus be considered as a satisfactory matrix alteration tracer. No significant burnup effect was observed on the alteration of the UO_2 fuel matrix. The daily strontium release factor was approximately $2.7\times10^{-8}\ \mathrm{d^{-1}}$ for UO_2 fuel after 706 days of leaching, and seven to eight times higher for MOX fuel. Several alteration mechanisms (radiolysis, solubility, precipitation/clogging) are examined to account for the experimental findings. All the available experimental data (characterization of secondary phases and leaching data) indicate that the mechanism limiting the spent fuel alteration kinetics, for the conditions studied, is likely based on the transport and accessibility of oxidizing species and/or water within the segment.

1. Introduction

For a potential performance assessment of direct disposal of spent fuel in a nuclear waste repository, the chemical reactions between the fuel and possible intruding water must be understood and the resulting radionuclide release must be quantified. Two source terms are distinguished today [1,2]: (i) Radionuclides that are not retained in the UO_2 fuel matrix can be released instantaneously when the fuel comes into contact with water. This source term, also known as the Instant Release Fraction, concerns the radionuclide inventories located at grain boundaries, in the gap, fractures and the rim, and is highly dependent on the physical condition of the fuel when it is exposed to water [1,2]. Long-term modeling of this radionuclide release requires a microscopic-level understanding of the mechanisms liable to modify the physical condition of the fuel prior to water ingress (grain decohesion, evolution of the inventories over time due to diffusion under alpha self-irradiation, etc.). (ii) The second source term covers the release of radionuclides from the UO_2 fuel matrix. Long-term modeling of this type of release implies that the mechanisms controlling the alteration kinetics of UO_2 grains exposed to water and radiation must be known and identified. Several mechanisms could control the matrix alteration over time, including radiolysis, interface solubility, or the protective effect of a precipitated phase.

This ongoing study was initiated five years ago to assess the influence of two parameters (fuel burnup and

---

* Corresponding author. Tel.: +33-4 66 79 16 42; fax: +33-4 66 79 77 08.

E-mail address: christophe.jegou@cea.fr (C. Jégou).

0022-3115/$ - see front matter © 2004 Elsevier B.V. All rights reserved.
doi:10.1016/j.jnucmat.2004.01.008

initial chemical composition) on the matrix alteration kinetics (second source term). The experimental results also provide evidence concerning the nature of the mechanisms (oxidizing dissolution controlled by radiolysis, growth of a protective layer controlled by solubility, etc.) liable to control matrix dissolution in aerated media. This study was the subject of an article presented at the MRS 2000 meeting by Jégou et al. [3], describing the first 313 days of leaching. Samples taken at later intervals have been analyzed since then, and a leached fuel specimen has been characterized by optical and electron microscopy to identify the resulting secondary phases.

2. Experimental approach

2.1. Fuel specification and characterization

Leaching experiments were performed with five spent fuel samples from French power reactors (Table 1):

- four UO_2 fuel samples with burnup ratings of 22, 37, 47 and 60 $GW\,d\,t_{HM}^{-1}$ (corresponding to 1, 3, 4 and 5 irradiation cycles, respectively);
- one MOX fuel sample irradiated to 47 $GW\,d\,t_{HM}^{-1}$ (3 irradiation cycles).

Two of these fuel samples (MOX and 5-cycle UOX) were characterized by electron microprobe analysis, scanning electron microscopy (SEM) and metallographic examinations before leaching.

2.2. Leaching experiments

Fig. 1 summarizes the leaching history of the fuel specimens. As the objective was to investigate the alteration of the spent fuel matrix, the test specimens (20 mm segments of clad fuel rods) were first washed (over a 3-year period) in static mode, in aerated carbonated groundwater (Table 2) at room temperature (25 °C) in a hot cell to remove the transferable activity (gap and grain boundary releases). Following this preliminary leaching phase, the fuel segments were transferred to sealed stainless steel leaching pots containing fresh carbonated groundwater for fuel matrix leaching tests. Solution samples were taken at regular intervals (8, 14, 21, 28, 64, 126, 194, 253, 313, 417, 545, 706 days) for radiochemical separation and β-counting for ^{90}Sr, γ-spectrometry for cesium (^{134}Cs and ^{137}Cs) and ICP-AES analysis for uranium. The solution samples were not filtered before uranium assay. The hydrogen peroxide (H_2O_2) concentration formed by radiolysis in the water was measured in the leachates by UV–visible spectrophotometry using Ghormley's method [4].

Only the leaching experiment on a spent fuel segment with a burnup of 60 $GW\,d\,t_{HM}^{-1}$ was terminated to characterize the sample after leaching (1000 days); the other fuel leaching experiments are still in progress. The spent fuel segment with a burnup of 60 $GW\,d\,t_{HM}^{-1}$ was characterized by optical and scanning electron microscopy (SEM) coupled with energy dispersive X-ray spectroscopy (EDX) microanalysis.

2.3. Solution analysis results

For a radionuclide X, the inventory fraction released into the aqueous phase (FIAP) is expressed as follows:

$$\mathrm{FIAP}_X = \frac{a_X^{\mathrm{sol}} V}{A_X^{\mathrm{inv}} f_{\mathrm{U}} m_{\mathrm{UO_2}}},$$

where a_X^{sol} is the activity (Bq ml^{-1}) of radionuclide X in aqueous phase in the leachate; A_X^{inv}, the specific activity (Bq $g_{(U)}^{-1}$) of radionuclide X in initial spent fuel inventory; V, the initial leachate volume (ml); $m_{\mathrm{UO_2}}$, the initial

Table 1
Spent fuel irradiation characteristics

Specimen batch	PWR UO_2 22 $GW\,d\,t_{HM}^{-1}$	PWR UO_2 37 $GW\,d\,t_{HM}^{-1}$	PWR UO_2 47 $GW\,d\,t_{HM}^{-1}$	PWR UO_2 60 $GW\,d\,t_{HM}^{-1}$	PWR MOX 47 $GW\,d\,t_{HM}^{-1}$
Reactor	Bugey 3	Bugey 3	Fessenheim 2	Gravelines 2	St Laurent B1
Fuel assembly	FGA 54	FGC 53	FEC 57	FF06E3BV	FFPOOHJX
Position in assembly	H 09	J 09	H 11	J 07	L 14
Initial ^{235}U enrichment	2.1 wt%	3.1 wt%	3.1 wt%	4.5 wt%	–
Initial (Pu/U + Pu) enrichment	–	–	–	–	5.6 wt%
Reactor cycles	1	3	4	5	3
Irradiation history	31 Aug. 78 to 14 Sept. 80	31 Aug. 78 to 4 Feb. 82	27 June 77 to 4 Jan. 83	20 Nov. 83 to 6 May 89	Dec. 87 to Jan. 91
Mean burnup ($GW\,d\,t_{HM}^{-1}$)	20.4	35.2	45.79	57.6	41.3

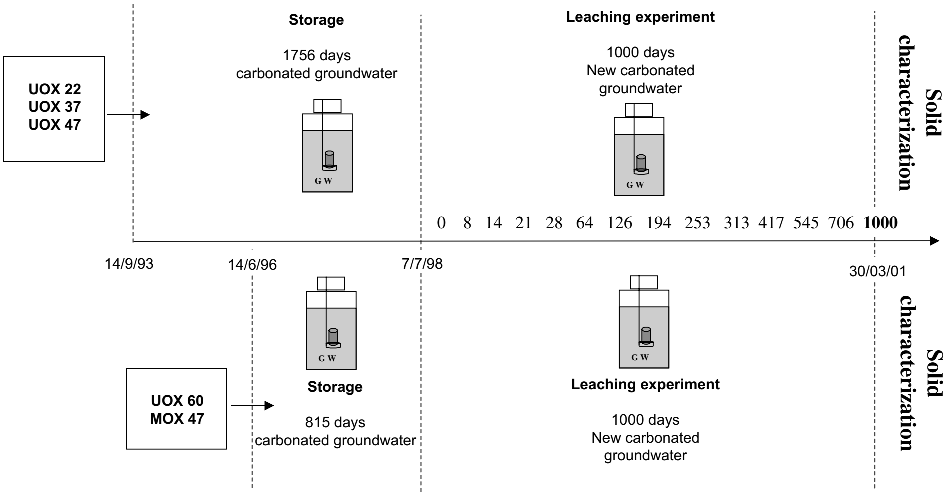

Fig. 1. Fuel sample leaching history.

Table 2
Chemical composition of the water

Chemical composition	Concentration ($mg\,L^{-1}$)	Concentration ($mol\,L^{-1}$)
SiO_2	23	3.8×10^{-4}
Ca	9.8	2.4×10^{-4}
Na	9.2	4.0×10^{-4}
Mg	5.4	2.2×10^{-4}
K	5.5	1.4×10^{-4}
Mn	<0.002	$<3.6\times10^{-8}$
Fe	<0.005	$<9.0\times10^{-8}$
F	0.21	1.1×10^{-5}
Cl	7	2.0×10^{-4}
P	2.7	8.6×10^{-5}
SO_4	7.2	7.5×10^{-5}
HCO_3	65.9	1.1×10^{-3}
As	0.015	2.0×10^{-7}
Pb	<0.005	$<2.4\times10^{-8}$
Zn	<0.03	$<4.6\times10^{-7}$
Cu	<0.002	$<3.1\times10^{-8}$
N	1	7.1×10^{-5}
CO_2	19.7	4.5×10^{-5}
pH	7.2	

oxide mass (g) in spent fuel specimen and f_U is the UO_2/U mass conversion factor: 0.8815 g of uranium metal per gram of UO_2. [1]

During the experiment, as the samples were analyzed at regular intervals, an average fraction release rate (FRR_a) (d^{-1}) between two time intervals can be determined from the differences between the released fractions at each interval:

$$\mathrm{FRR_a}X(n) = \frac{\mathrm{FIAP}_X(n) - \mathrm{FIAP}_X(n-1)}{t_n - t_{n-1}}.$$

The release rates defined here do not take into account the reactive surface area of the sample, and thus provide no indication of the alteration rate per unit area. Given the sample surface area accessible to water, the alteration rate R ($g\,m^{-2}\,d^{-1}$) could be determined from the following relation:

$$R = \mathrm{FRR_a}\frac{m_{UO_2}}{S}.$$

Nevertheless, the geometric surface area of the test fuel sections was estimated to obtain representative alteration rate values.

3. Results

3.1. Strontium release

After 706 days of leaching, the strontium inventory fractions released into solution were comparable for all the UOX fuel samples, ranging from 5×10^{-5} to 10^{-4} (Fig. 2).

Different behavior was observed for MOX fuel: the Sr release was 5–6 times greater than for UOX fuel with a burnup of $60\,\mathrm{GW\,d\,t_{HMi}^{-1}}$. The fraction entering solution reached 3.2×10^{-4} for the MOX fuel sample after 706 days of leaching (Fig. 2).

Fig. 3 compares the evolution of the daily Sr fractions released over the duration of the experiment. For greater clarity, only three of the fuel samples studied

---

[1] The heavy metal quantity taken into account for MOX includes the plutonium; the same conversion factor is used.

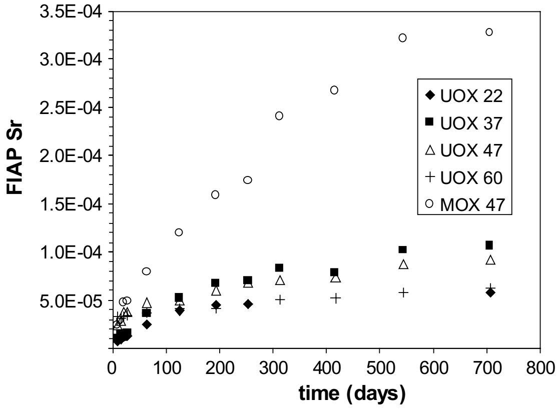

Fig. 2. Cumulative released strontium fractions.

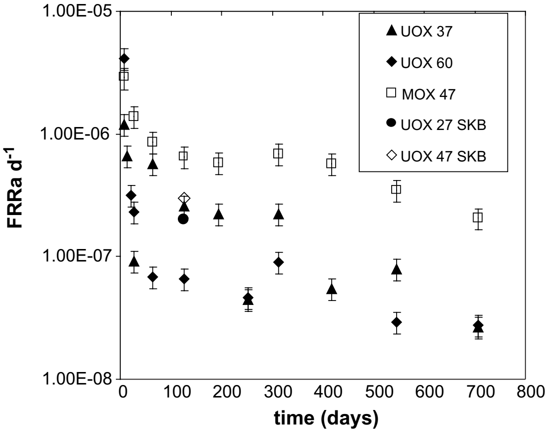

Fig. 3. Average fractional release rate FRR_a (d^{-1}) for strontium.

(UOX 60 + UOX 37 + MOX 47) are shown here. The release rate continued to diminish over time, reaching a value of 3×10^{-8} d^{-1} for all the UOX fuel samples after 706 days of leaching. The Sr release rate from MOX fuel was 2×10^{-7} d^{-1}, and remained seven to eight times higher than for the UOX fuel samples (Table 3). Fig. 3 also shows the results obtained by Forsyth et al. [5,6] under the same experimental conditions (carbonated groundwater at 25 °C) for fuel samples with burnup values ranging from 27 to 48 $\mathrm{GW\,d\,t_{HM}^{-1}}$. The results of both series of experiments were fully comparable.

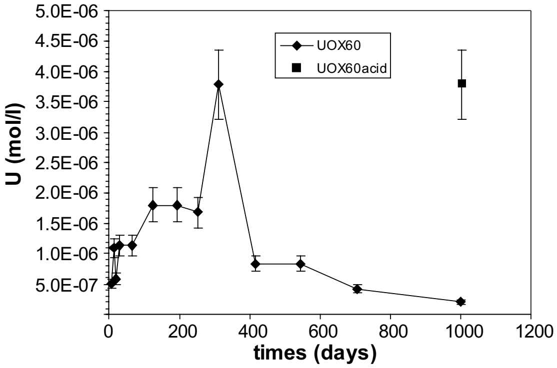

Fig. 4. Uranium concentration measured by ICP-AES in spent fuel leachates.

3.2. Uranium release

Fig. 4 shows the uranium concentration in solution versus time for UOX 60 fuel. Up to 313 days, the uranium concentration increased to about 4×10^{-6} mol L^{-1}. The concentration then suddenly dropped. It has to be noted that (i) the sampling vessels were not agitated, which means the solution may not be completely homogeneous (formation of polynuclear species or colloids), (ii) samplings were performed using needle introduced at the middle of the leaching vessel. At the end of the experiment, after removal of the spent fuel segment from the vessel for characterization, the leachate was acidified. Analysis of the acidified leachate indicated the same concentration as after 313 days of leaching. These results seem to infer that the total amount of uranium released to the solution was roughly constant between 313 days and the end of the experiment but include either some non soluble species (sorption of the walls, poorly-crystallized secondary phases...) or some colloidal forms preferentially located at the bottom of the vessel.

3.3. Cesium release

Fig. 5 shows the variation over time of the cesium inventory fraction released into solution for two fuels

Table 3
Spent fuel activity (Bq g^{-1}) and fraction release rates (d^{-1}) after 706 days

	UOX 22	UOX 37	UOX 47	UOX 60	MOX 47
α activity	1.6×10^8	3.4×10^8	5.7×10^8	9.0×10^8	25.5×10^8
βγ activity	5.6×10^9	9.7×10^9	11.2×10^9	18.1×10^9	27.0×10^9
FRR(Sr)	2.7×10^8	2.7×10^8	2.5×10^8	2.75×10^8	2.0×10^7

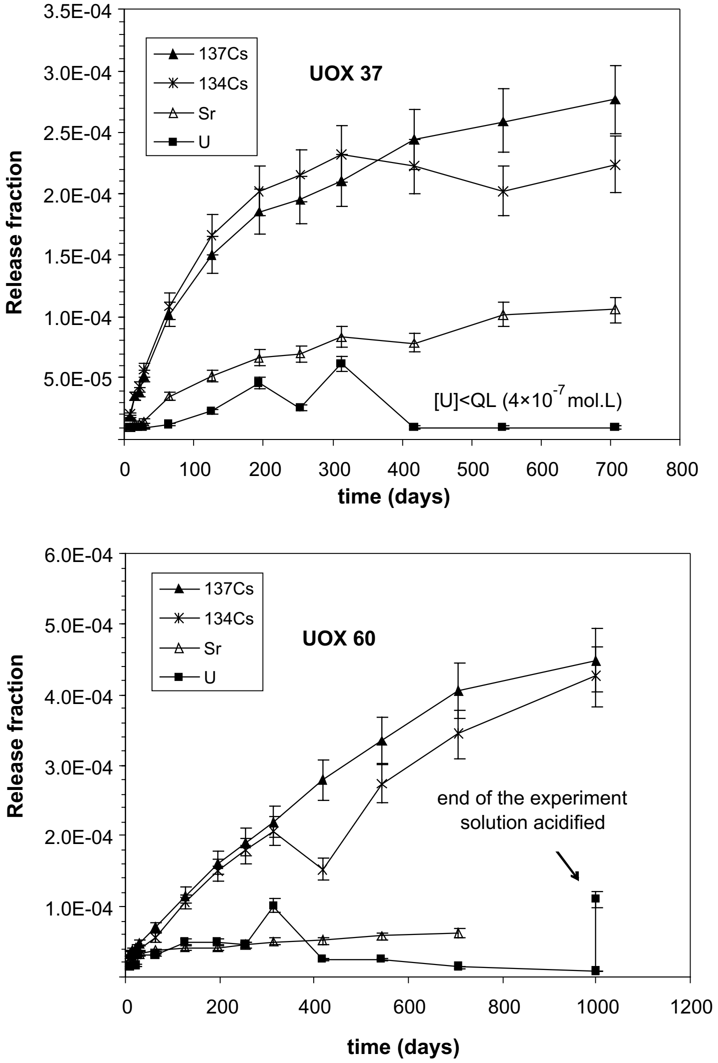

Fig. 5. Cumulative released cesium fractions.

(UOX 37 and UOX 60). The released strontium and uranium fractions are also shown to highlight the differences in behavior. The cesium release was generally much greater than the uranium and strontium release indicating a possible attack at grain boundaries enriched in migrated cesium (migration of cesium during irradiation) [6]. The released fractions after 706 days ranged from 2.5×10^{-4} to 4.5×10^{-4}.

3.4. Sr/U and Cs/U congruence ratios

The $FIAP_{Sr}/FIAP_{U}$ congruence ratios were calculated for all the fuel samples; the mean values until 313 days are indicated in Table 4. The results ranged from 1 to 2 for all the UOX fuel samples, and were about 3 times higher for the MOX fuel. These congruence ratios were determined below uranium saturation: the 313-day uranium concentrations did not exceed 4.0×10^{-6} $mol\,L^{-1}$, close to the solubility of schoepite (a kinetically favored secondary phase) and the values obtained by SKB (about 10^{-5} $mol\,L^{-1}$) [5,6] in similar carbonated groundwater over longer periods. It should be noted that the uranium concentrations were determined after

Table 4
Mean $FIAP_{Sr}/FIAP_{U}$ ratio until 313 days of leaching under unsaturated conditions

UOX 22	UOX 37	UOX 47	UOX 60	MOX 47
2.1	1.6	1.9	1.2	5.6

acidifying the samples, and thus take into account any colloidal species in solution. Beyond 313 days, the $FIAP_{Sr}/FIAP_U$ ratios increased in all the fuel samples, from 1.6 to 10 for UOX 37 and from 1.2 to 4.5 for UOX 60 (Fig. 6).

The $FIAP_{Cs}/FIAP_U$ congruence ratios exhibited the same variation as the $FIAP_{Sr}/FIAP_U$ ratios. Beyond 313 days they increased from 5 to 25 for UOX 37 fuel and from 2.5 to 55 for UOX 60 fuel (Fig. 6). Before 313 days the $FIAP_{Cs}/FIAP_U$ ratios remained significantly above 1, unlike the $FIAP_{Sr}/FIAP_U$ ratios.

3.5. Hydrogen peroxide determination

The H_2O_2 concentration in the leachate was measured using Ghormley's method, in which H_2O_2 reacts with excess iodide ions to form a triiodide complex anion, the concentration of which is determined by spectrophotometry ($OD = \varepsilon cl$, where $\varepsilon \approx 23400$ $mol^{-1}\,L\,cm^{-1}$ at 350 nm). The optical densities were very low for all the samples, and the H_2O_2 concentrations were *below* the determination limit of this method (4×10^{-6} $mol\,L^{-1}$) after 706 days of leaching.

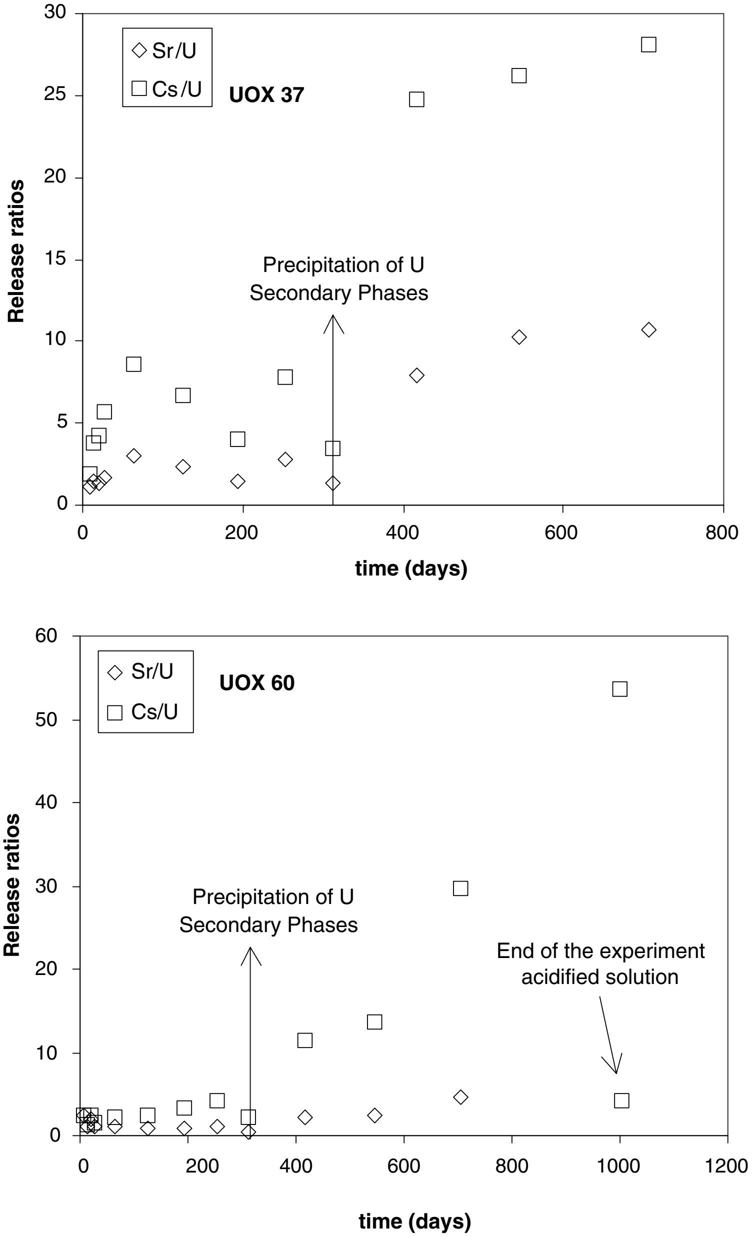

Fig. 6. $FIAP_{Sr}/FIAP_U$ and $FIAP_{Cs}/FIAP_U$ ratios versus time.

4. Discussion and effect on the fuel matrix alteration kinetics of secondary phases formed on the surface of the fuel segment in aerated media

4.1. Strontium data as an indicator of matrix behavior

The $FIAP_{Sr}/FIAP_U$ congruence ratios (Table 4) show that strontium is a suitable matrix alteration tracer for UOX fuel after elimination of the instantaneous release fraction. After 313 days of leaching it is still possible to follow the UOX fuel matrix alteration kinetics from the strontium release, given that the sudden rise in the $FIAP_{Sr}/FIAP_U$ ratio corresponds to significant uranium colloids formation and/or sorption, and that uranium can then no longer be used as an alteration tracer.

Considering the heterogeneous chemical composition of MOX fuel and in particular the differences in the strontium distribution between plutonium-rich agglomerates (0.15 wt% Sr) and the remainder of the matrix (0.06 wt% Sr) (Fig. 7), it is difficult to assess the significance of the ratio of 5.6 obtained for MOX fuel.

4.2. UOX/MOX comparison

The mean strontium release rate was some seven times higher in the MOX fuel sample than in the UOX samples (Fig. 3). Several factors could account for this difference:

- the greater reactive surface area of MOX fuel arising from its highly porous 'cauliflower' structure in the plutonium-rich agglomerates with locally high burnup;
- concentration of the strontium and cesium inventory in the plutonium-rich agglomerates, in conjunction with preferential leaching of these agglomerates;
- greater alteration of the $(U,Pu)O_2$ matrix.

It is difficult to identify the most likely hypothesis at this time. ICP-MS and ICP-AES studies of Pu, U, Sr and Cs release in leaching experiments of short duration or under dynamic conditions will provide data on the origin of the released inventory (agglomerates, UO_2 matrix).

4.3. Mechanisms liable to control oxide matrix dissolution

The fuel matrix dissolution kinetics in oxidizing media can be controlled by various mechanisms proposed by Grambow et al. [7]:

- generation of oxidizing species by water radiolysis,
- surface reaction and solubility of the oxidized surface,
- growth of a secondary phase or alteration product on the surface,
- oxygen and/or water transport to the surface.

Each of these mechanisms can be discussed in the light of the results obtained (leaching data and surface characterization of the UOX 60 fuel segment after leaching).

4.3.1. Generation of oxidizing species by water radiolysis

Assuming the alteration kinetics are expressed as the product of a kinetic constant and a concentration of oxidizing species ($R = k[\mathrm{Ox}]$), the kinetics will be affected by the concentration of oxidizing species at the UO_2/UO_{2+x} interface.

Table 3 shows the fraction release rates and the αβγ activities of the fuel samples with burnup values ranging from 22 to 60 $\mathrm{GW\,d\,t_{HM}^{-1}}$ as calculated using the CESAR code [8]; the activity increases with the burnup. If the concentration of oxidizing species follows the increasing fuel activity, the alteration rate ($R = k[\mathrm{Ox}]$) should also rise with the burnup. Moreover, as the initial surface area accessible to water most likely increases with the burnup (except for UOX 60 fuel in which the oxide/clad gap was filled), the product RS should follow the same trend. This is in contradiction with our experimental

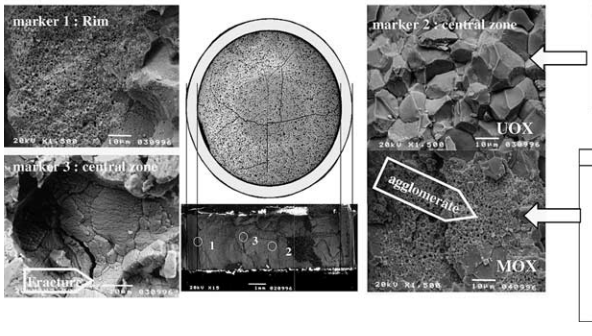

Element	UOX
Pu	1.0
Nd	0.5
Zr	0.4
Sr	<600ppm RIM : 1000ppm
Cs	0.4

Element		MOX
Pu	Matrix	1.5
	Agglomerate	12 à 15
Nd	Matrix	0.2
	Agglomerate	1.3
Zr	Matrix	0.2
	Agglomerate	1.3
Sr	Matrix	<600ppm
	Agglomerate	until 0.15 %
Cs	Matrix	0.25
	Agglomerate	0.7 à 1

Fig. 7. Results of characterization by electron microprobe analysis, scanning electron microscopy (SEM) and metallographic examinations (before leaching).

observation of a constant RS value (Table 3). As the experiments were conducted in aerated media, the effects of water radiolysis were probably masked by the presence of oxygen and $R = k[\mathrm{Ox}]$ was probably similar for all the fuel samples. This hypothesis is supported by the low H_2O_2 concentrations measured in the fuel leachates ($<4\times10^{-6}$ mol L^{-1}), and should be considered in the light of the SKB experiments [5,6] conducted in aerated and deaerated media, showing 4 times greater release with aeration.

4.3.2. *Surface reaction and solubility of the oxidized surface*

The matrix alteration could be limited by the dissolution of the oxidized surface layer UO_{2+x}. The dissolution rate of the oxidized layer can be expressed by a chemical affinity law of the following type [7]:

$$R_{\mathrm{diss}(2)} = r_0\left(1 - \frac{C}{C^*_{\mathrm{UO}_{2+x}}}\right),$$

where r_0 is the initial dissolution rate, C is the uranium concentration in solution, and $C^*_{\mathrm{UO}_{2+x}}$ is the solubility limit of the oxidized phase at the surface of the material.

If a kinetic law of this type is valid, the alteration rate should remain constant at r_0 when far from uranium saturation. The strontium release rate should also drop as uranium approaches saturation. Fig. 8 clearly shows that such behavior is not observed experimentally and that the strontium release is not directly correlated with uranium solubility. The drop in the fuel matrix alteration rate therefore cannot be described by a law of this type.

Moreover, the experimental evidence after 313 days of a drop in the uranium concentration together with continued alteration of the fuel matrix suggests the formation of secondary uranium U(VI) phases (schoepite, Na-polyuranates, becquerellite, alteration products including either the silicate or the phosphate ligands,...?), more thermodynamically stable than the fuel with respect to the alteration solution.

A UOX 60 fuel segment was characterized by optical and electron microscopy to confirm this hypothesis. The fuel segment was observed along a cross section (leached sections + internal section). The main results are discussed below. Fig. 9 reveals the presence of secondary phases (yellow and green precipitates) in the fractures and on the open section of the segment subjected to

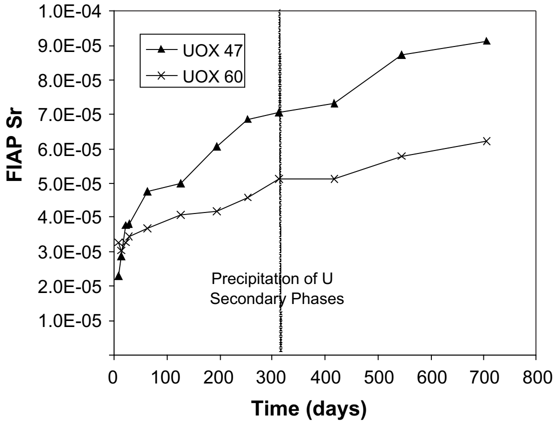

Fig. 8. Cumulative released strontium fractions for UOX 47 and UOX 60.

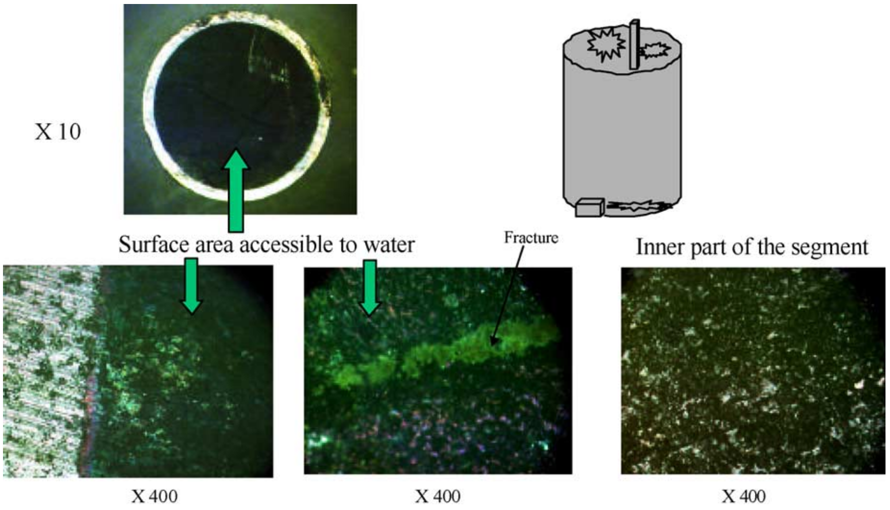

Fig. 9. Optical micrographs of a leached section and an internal section of the UOX 60 fuel segment.

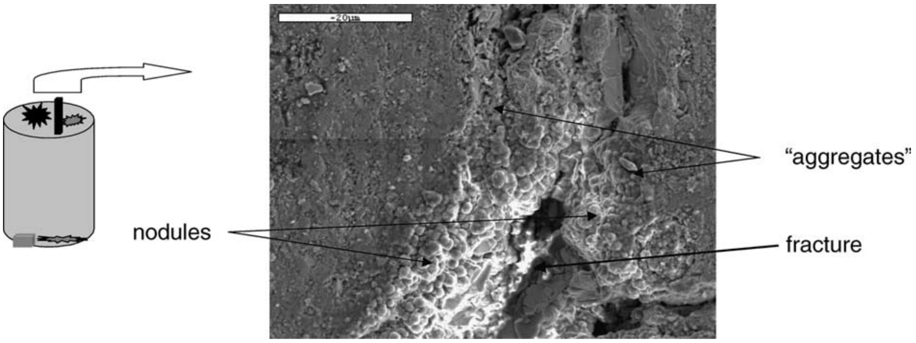

Fig. 10. Electron micrograph of a fracture. Nodules and aggregates were observed in the fracture and over the entire leached section (the white bar represents 20 μm).

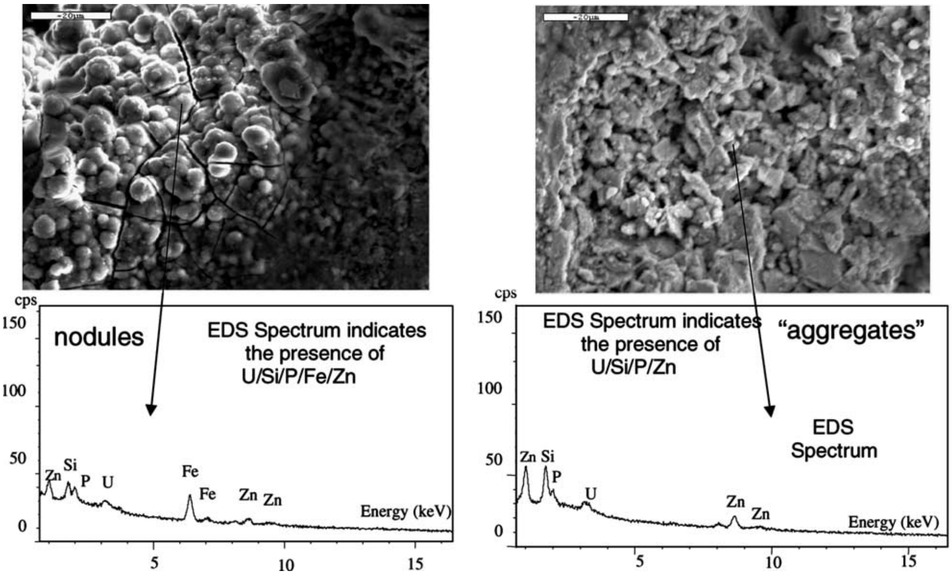

Fig. 11. EDS spectra of nodules and ‘aggregates’.

aqueous alteration. [2] An examination of the internal section does not show any significant difference with an unleached fuel sample; this suggests that water and/or oxidizing species did not reach the core of the segment after several years of alteration.

Fig. 10 more clearly shows the morphology of the precipitates, consisting of nodules and aggregates with similar chemical compositions. The EDS spectra reveal the presence of Si, U, P, Zn and Fe on the surface of the fuel (Fig. 11). The presence of Na was confirmed by electron microprobe analysis.

The elements detected in the alteration film came in part from the alteration solution (notably Si, Na and P: see Table 2). Iron and zinc were attributable to pollution by the stainless steel leaching vessel and by the solution sampling needle. Precipitation formed only a surface layer, as shown by the fact that only uranium (UO_2) grains were detected in some scraped sites (Fig. 12). It is difficult to estimate the thickness of this alteration layer from observation of the leached sections. It should be possible to determine the alteration depth by analysis of silicon (for example) lengthwise within the segment.

Thermodynamic calculations were performed using the JCHESS geochemical code [9] with the thermodynamic data base from the EQ3/6 code [10] to determine

---

[2] For interpretation of color in Fig. 9, the reader is referred to the web version of this article.

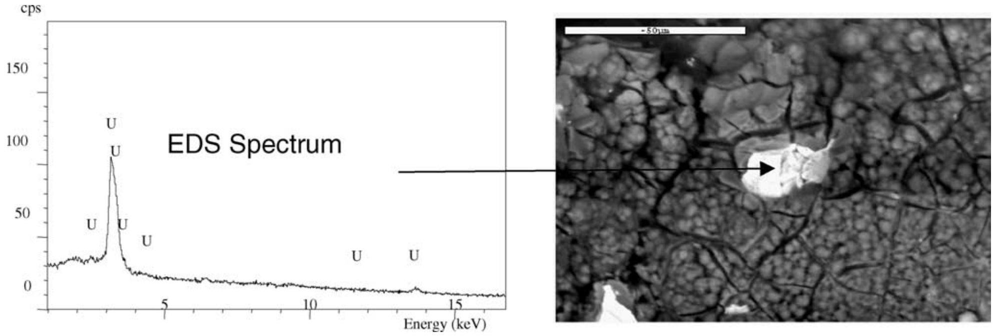

Fig. 12. BSE image of the leached surface revealing the presence of UO_2 grains beneath the alteration film (the white bar represents 50 µm).

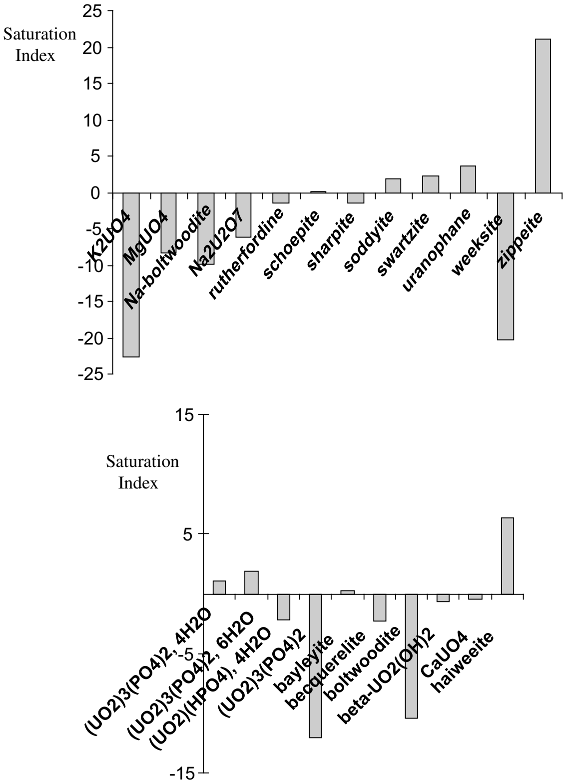

Fig. 13. Saturation index for uranium phases.

the nature of the phases containing U(VI) liable to precipitate in aerated media. Fig. 13 shows the calculated saturation indexes for various phases. The saturation indexes for uranium phosphates and for some uranium silicates (including uranophane and soddyite) are positive, suggesting that these phases may have precipitated in accordance with the surface elemental analysis findings.

Several calcium precipitates were also observed on the surface open section of the segment as shown in Fig. 14.

4.3.3. Growth of a secondary phase or alteration product on the surface

Characterization of the segment revealed the presence of secondary phases and an alteration layer consisting in particular of uranium and silicon; this raises the issue of control of the fuel alteration kinetics based on the growth of the alteration layer.

The growth of this layer would consume uranium, disturbing the local equilibrium between the solution and the UO_{2+x} fuel surface. The strontium release rate would then be constant or would increase with the reactive surface area of the precipitating phase. As the experimentally determined strontium release rate continues to diminish in all the fuel samples, this hypothesis must also be rejected.

4.3.4. Oxygen and/or water transport to the surface

The alteration film could also control the fuel matrix alteration kinetics:

- by forming a diffusion barrier (with respect to oxidizing species and/or water) – i.e. a passivating film – on the UO_2 surface,
- by sealing the pores and cracks, and thus limiting the accessibility of water and oxidizing species to the core of the segment (reducing the reactive surface area over time).

Fig. 15 shows a linear relation between the strontium release and the square root of time for UOX fuel. Unlike the initial interpretations based on the first 313 days of leaching [3], for which a relation between strontium release and time (or $\sqrt{t}$) could not be positively identified, the data available up to 706 days appear to confirm a relation with $\sqrt{t}$ (Fig. 16). Assuming

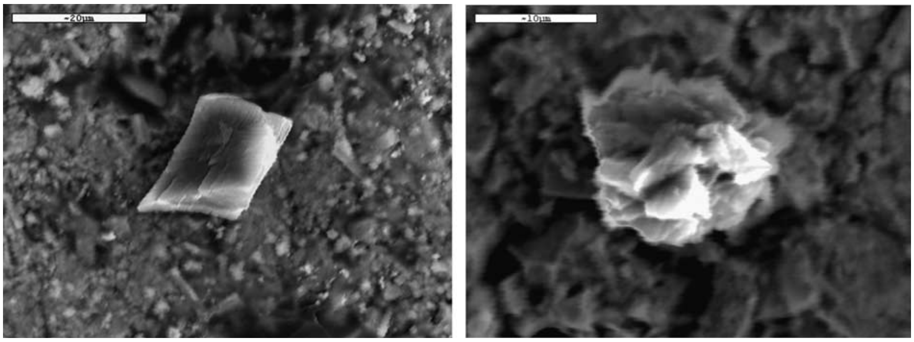

Fig. 14. Calcium precipitates (the white bar represents 20 µm).

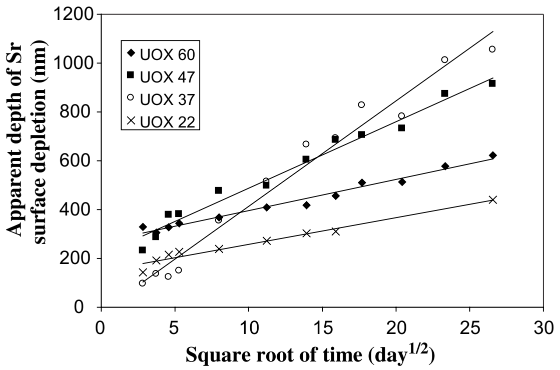

Fig. 15. Apparent depth of Sr surface depletion (nm) versus the square root of time.

only the open ends of the segments were altered, it is then possible to calculate a strontium alteration thickness and a diffusion coefficient based on the relation $e = \sqrt{Dt}$ (Fig. 15). Thus $D_{\text{calc}} \approx 10^{-20}\ \text{m}^2\,\text{s}^{-1}$ at 25 °C.

Although the nature of the mechanism controlling fuel matrix alteration has not been clearly established (passivation or sealing), the available experimental data (characterization + leaching data) point to a limiting mechanism based on transport.

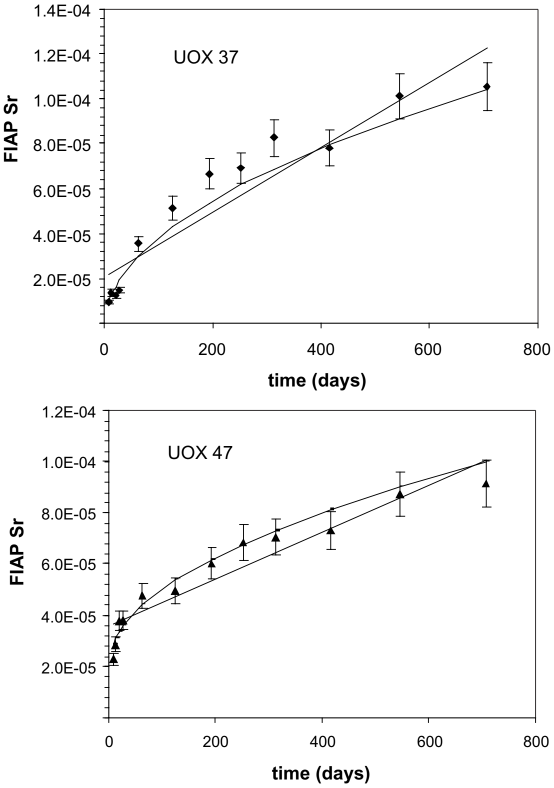

Fig. 16. Released strontium inventory fractions versus the time for UOX 37 and UOX 47.

4.4. Surface area accessible to water – estimated alteration rate

The geometric surface area of a spent fuel section can be estimated from the lateral area ($S_{\text{l}} = 5.146\ \text{cm}^2$) and the end-face area ($S_{\text{e}} = 1.054\ \text{cm}^2$) [5,6,11]; the area due to fracturing is not taken into account. As the oxide/clad gap was nil in the UOX 60 sample, its reactive surface area was limited to the open ends of the chopped sections (disregarding fracturing). However, the strontium release rate for this sample was similar to the rates observed for the other UOX fuel samples, suggesting that precipitation tends to be localized in the oxide/clad gap, limiting the accessible surface area to the open ends of the sections in all cases. This hypothesis was already considered by Forsyth et al. [5] to account for the reductions and differences in the release rates observed over time for fuel fragments and sections.

A UOX fuel matrix alteration rate *R* can be calculated by limiting the reactive surface area to the open end faces alone, and by applying a correction factor of

Table 5
UOX fuel dissolution rate ($mg\,m^{-2}\,d^{-1}$) calculated by considering only the geometric surface area at the ends of the fuel sections (this work and [5]) and with powder fuel samples [12]

This work	[5]	[12]
1–2 $mg\,m^{-2}\,d^{-1}$	0.6–6 $mg\,m^{-2}\,d^{-1}$	2 $mg\,m^{-2}\,d^{-1}$

3 to taken account of surface irregularities [4]. Table 5 indicates the matrix alteration rates obtained in this study, together with the comparable values reported by Forsyth [5] and Gray [12] for fuel sections and fragments.

5. Conclusions

The experimental results presented here show that strontium is a suitable matrix alteration tracer for UOX fuel once the instantaneous release fraction has been leached. The $FIAP_{Sr}/FIAP_U$ ratio, which remains high and exceeds 1 for MOX fuel, suggests preferential alteration of the aggregates.

No significant burnup effect was observed on the alteration of the UO_2 fuel matrix. The daily strontium release factor was approximately $2.7 \times 10^{-8}\ d^{-1}$ for UO_2 fuel, and seven to eight times higher for MOX fuel after 706 days of leaching.

Various alteration mechanisms have been considered to account for the experimental findings. All the available experimental data (characterization of secondary phases + leaching data) indicate that the mechanism limiting the spent fuel alteration kinetics, for the conditions studied, is likely based on the transport and accessibility of oxidizing species and/or water within the segment. The formation and identification of the secondary phases liable to limit this transport constitute an area in which further research is necessary.

Acknowledgements

Financial support for this research has been provided in the framework of the CEA-PRECCI program (C. Poinssot and C. Ferry) as part of CEA-EDF (J.M. Gras) agreement.

The authors gratefully acknowledge the contributions of the staff of Atalante (DHA) Hot Cell Laboratory.

References

[1] C. Poinssot, C. Jégou, P. Toulhoat, J.-P. Piron, J.-M. Gras, Mater. Res. Soc. Symp. Proc. 663 (2002) 469.
[2] C. Poinssot, P. Lovera, M.H. Faure, Mater. Res. Soc. Symp. Proc. 713 (2002) 615.
[3] C. Jégou, S. Peuget, J.F. Lucchini, C. Corbel, V. Broudic, J.M. Bart, Matrix Mater. Res. Soc. Symp. Proc. 663 (2002) 399.
[4] Hochanadel, J. Phys. Chem. 56 (1952) 587.
[5] R.S. Forsyth, The SKB spent fuel corrosion program, SKB Technical Report 97-25, December 1997.
[6] R.S. Forsyth, L.O. Werme, J. Nucl. Mater. 190 (1992) 3.
[7] B. Grambow, L.O. Werme, R.S. Forsyth, J. Bruno, Mater. Res. Soc. Symp. Proc. 176 (1990) 465.
[8] J.P. Grouiller, J. Pavageau, Synthesis on the spent nuclear fuel evolution, CEA R-5958 report, 2001, 616 p (ISSN0429-3460).
[9] J. Van Der Lee, L. De Windt, CHESS Tutorial and Cookbook, Updated for version 3.0, Users manual Nr LHM/RD/02/13, École des Mines de Paris, Fontainebleau, France, 2002.
[10] T.J. Wolery, EQ3/6: a software package for geochemical modeling of aqueous systems: package overview and installation guide (version 7.0), UCRL-MA-110662 PT I ed., Lawrence Livermore National Laboratory, 1992.
[11] A. Loida, B. Grambow, H. Geckeis, J. Nucl. Mater. 238 (1996) 11.
[12] W.J. Gray, D.M. Strachan, Mater. Res. Soc. Symp. Proc. 212 (1991) 205.